Water Research 80 (2015) 20–29

Contents lists available at ScienceDirect

Water Research

journal homepage: www.elsevier.com/locate/watres

Mechanisms of enhanced total organic carbon elimination from oxalic acid solutions by electro-peroxone process

Huijiao Wang [a], Shi Yuan [a], Juhong Zhan [a, b], Yujue Wang [a, *], Gang Yu [a], Shubo Deng [a], Jun Huang [a], Bin Wang [a]

[a] School of Environment, Beijing Key Laboratory for Emerging Organic Contaminants Control, State Key Joint Laboratory of Environmental Simulation and Pollution Control, Tsinghua University, Beijing, 100084, China

[b] Faculty of Environmental Science and Engineering, Kunming University of Science and Technology, Kunming, Yunnan, 650500, China

ARTICLE INFO

Article history:
Received 3 November 2014
Received in revised form
24 April 2015
Accepted 12 May 2015
Available online 14 May 2015

Keywords:
Advanced oxidation
Ozone
Hydrogen peroxide
Electrocatalytic ozonation
Electrolysis

ABSTRACT

Electro-peroxone (E-peroxone) is a novel electrocatalytic ozonation process that combines ozonation and electrolysis process to enhance pollutant degradation during water and wastewater treatment. This enhancement has been mainly attributed to several mechanisms that increase O_3 transformation to •OH in the E-peroxone system, e.g., electro-generation of H_2O_2 from O_2 at a carbon-based cathode and its subsequent peroxone reaction with O_3 to •OH, electro-reduction of O_3 to •OH at the cathode, and O_3 decomposition to •OH at high local pH near the cathode. To get more insight how these mechanisms contribute respectively to the enhancement, this study investigated total organic carbon (TOC) elimination from oxalic acid (OA) solutions by the E-peroxone process. Results show that the E-peroxone process significantly increased TOC elimination rate by 10.2–12.5 times compared with the linear addition of the individual rates of corresponding ozonation and electrolysis process. Kinetic analyses reveal that the electrochemically-driven peroxone reaction is the most important mechanism for the enhanced TOC elimination rate, while the other mechanisms contribute minor to the enhancement by a factor of 1.6–2.5. The results indicate that proper selection of electrodes that can effectively produce H_2O_2 at the cathode is critical to maximize TOC elimination in the E-peroxone process.

1. Introduction

Ozone (O_3) has been widely used in water and wastewater treatment as an oxidant for decades. Due to its high oxidation potential, O_3 can rapidly degrade many pollutants, especially compounds with activated double bonds (e.g., activated aromatic systems, deprotonated amines, and reduced sulfur groups) (von Gunten, 2003; Hoigné and Bader, 1983). However, O_3 is also a highly selective oxidant, ozonation thus often results in the accumulation of many refractory oxidation by-products (e.g., aldehydes and carboxylic acids) that resist further O_3 oxidation in its effluents (Petre et al., 2013). Consequently, ozonation has often been shown to be ineffective at total organic carbon (TOC) abatement (von Gunten, 2003). This has restricted the application of ozonation when high TOC removal efficiency is desired to minimize the risks associated with degradation intermediates (e.g., in drinking water treatment and wastewater reclamation) (Petre et al., 2013; Vecitis et al., 2010).

To improve TOC removal, O_3 has often been used with other technologies such as UV, ultrasound, H_2O_2, and electrochemical processes (von Gunten, 2003; Weavers et al., 1998; Kishimoto et al., 2005; Yuan et al., 2013; Pines and Reckhow, 2002). These combinations can usually enhance O_3 transformation to hydroxyl radicals (•OH), which are a much stronger oxidant and can non-selectively oxidize most organics much faster than O_3. Consequently, pollutants can be degraded more rapidly in these combined processes than ozonation alone. Particularly, the combination of ozonation with electrolysis has gained increasing interest recently because electrolysis is a robust and environmentally-friendly technology and amenable to control and automation (Kishimoto et al., 2005; Yuan et al., 2013; García-Morales et al., 2013; Qiu et al., 2014).

In early combined ozonation and electrolysis processes (referred as O_3-electrolysis hereafter), metal electrodes were used as both the anode (e.g., Pt, RuO_2/Ti, and Pt/Ti) and cathode (e.g., stainless steel (SS), Ti, and Pt) (Kishimoto et al., 2005, 2007, 2008). During the

* Corresponding author.
E-mail address: wangyujue@tsinghua.edu.cn (Y. Wang).

http://dx.doi.org/10.1016/j.watres.2015.05.024
0043-1354/

O_3-electrolysis process, pollutants can be oxidized in the same way as in electrolysis alone, i.e., via direct electron transfer to the anode (i.e., direct electrolysis) and via chemical reactions with oxidants (e.g., HClO, $H_2S_2O_8$, and •OH) electrochemically generated at the anode (i.e., indirect electrolysis) (Panizza and Cerisola, 2009). In addition, pollutants can be oxidized in the O_3-electrolysis process by •OH generated from cathodically induced reactions, e.g., the electro-reduction of O_3 at the cathode (Eqs. (1)–(3)) (Kishimoto et al., 2005), as well as the decomposition of O_3 (Eqs. (4)–(6), (2), and (3) (von Sonntag and von Gunten, 2012; Merenyi et al., 2010a)) in the vicinity of the cathode, where the local pH is high due to OH^- formation from H_2 evolution. As a result of the enhanced •OH generation, the O_3-electrolysis process can considerably improve pollutant degradation (Kishimoto et al., 2005, 2007).

$$O_3 + e^- \rightarrow O_3^- \cdot \tag{1}$$

$$O_3^- \cdot \leftrightarrow O_2 + O^- \cdot \tag{2}$$

$$O^- \cdot + H_2O \leftrightarrow \cdot OH + OH^- \tag{3}$$

$$O_3 + OH^- \rightarrow HO_4^- \tag{4}$$

$$HO_4^- \leftrightarrow HO_2 \cdot + O_2^- \cdot \tag{5}$$

$$O_2^- \cdot + O_3 \rightarrow O_2 + O_3^- \cdot \tag{6}$$

More recently, boron-doped diamond (BDD) electrodes have been used to further enhance TOC removal in the O_3-electrolysis process (García-Morales et al., 2013; Qiu et al., 2014; Bakheet et al., 2014). Compared with metal electrodes, BDD electrode is more effective at producing •OH from water discharge (Eq. (7)) because it has an inert surface and high oxygen overpotential (Panizza and Cerisola, 2009). It is therefore mainly used as the anode to improve the oxidation of ozone-refractory compounds (e.g., carboxylic acid by-products formed) in the O_3-electrolysis process (Qiu et al., 2014; Bakheet et al., 2014).

$$BDD + H_2O \rightarrow BDD(\cdot OH) + H^+ + e^- \tag{7}$$

While the O_3-electrolysis process has considerably enhanced TOC elimination as compared to the two individual processes, we perceived that it still has vast potential for improvement. For example, ozone generators usually can convert only a small part of the feed O_2 gas to O_3. The gas mixture exiting ozone generators thus still contains significant amounts of O_2, e.g., usually >90% V/V of the O_2 and O_3 mixture when pure O_2 is used as the feed gas. However, O_2 has little use for pollutant removal after it is sparged with O_3 into the reactors. This wastes considerable amounts of O_2 feed gas and energy (e.g., for concentrating O_2 from air and sparging the gas into the reactor). We therefore proposed to utilize O_2 in the sparged gas to electro-generate H_2O_2 in the reactor (Eq. (8)), whose conjugated base (HO_2^-, Eq. (9)) can then react with the sparged O_3 to yield •OH (Eqs. (10), (11), (2) and (3)) (von Sonntag and von Gunten, 2012; Fischbacher et al., 2013; Merenyi et al., 2010b), and thus further enhance TOC elimination (Yuan et al., 2013). Because the reaction of O_3 with H_2O_2 has been commonly referred as the "peroxone" reaction, we have termed this electrochemically-driven process as "electro-peroxone" (E-peroxone) process (Yuan et al., 2013). Note that the overall peroxone reaction has previously been suggested as Eq. (12) (i.e., two •OH formed per H_2O_2 consumed). However, recent studies suggest that the efficiency of •OH formation is only one half of that given by the stoichiometry in Eq. (12) because HO_5^- (the adduct of O_3 with HO_2^-, Eq. (10)) undergoes decomposition to form O_2 and OH^- (Eq. (13)) at a comparable rate of Eq. (11) (Fischbacher et al., 2013).

$$O_2 + 2H^+ + 2e^- \rightarrow H_2O_2 \tag{8}$$

$$H_2O_2 \leftrightarrow H^+ + HO_2^- \tag{9}$$

$$HO_2^- + O_3 \rightarrow HO_5^- \tag{10}$$

$$HO_5^- \rightarrow HO_2 \cdot + O_3^- \cdot \tag{11}$$

$$H_2O_2 + 2O_3 \rightarrow 2 \cdot OH + 3O_2 \tag{12}$$

$$HO_5^- \rightarrow 2\,{}^3O^2 + OH^- \tag{13}$$

The E-peroxone process can be easily achieved by replacing the metal cathodes used in previous O_3-electrolysis processes with a carbon-based cathode. In contrast to metal electrodes that may catalytically decompose H_2O_2 and thus cannot produce H_2O_2 from O_2 (Yuan et al., 2013; Sudoh et al., 1985; Bakheet et al., 2013), carbon-based electrodes (e.g., carbon-polytetrafluorethylene (carbon-PTFE), carbon felt, and activated carbon fiber) can convert O_2 efficiently to H_2O_2 due to their high overpotential for H_2 evolution and low catalytic activity for H_2O_2 decomposition (Brillas et al., 2009; Wang et al., 2012; Panizza and Cerisola, 2001).

In previous work, we have evaluated the E-peroxone treatment of several different wastewaters, e.g., landfill leachate and synthetic dyes (Bakheet et al., 2013; Li et al., 2013). It was found that under similar reaction conditions (e.g., applied current and O_3 dose), the E-peroxone process removed TOC from the wastewaters much faster than ozonation, electrolysis, and the O_3-electrolysis process (Bakheet et al., 2013; Li et al., 2013; Wang et al., 2015). This enhancement has been mainly attributed to the significant production of •OH from several mechanisms in the E-peroxone process, e.g., the aforementioned electro-reduction of O_3, O_3 decomposition at high local pH near the cathode, and O_3 reaction with electro-generated H_2O_2 (Bakheet et al., 2013; Li et al., 2013; Wang et al., 2015). These cathodically-induced •OH can oxidize ozone-refractory compounds (e.g., saturated carboxylic acids) to CO_2, thus enhancing TOC removal from water. However, how these mechanisms contribute respectively to the enhancement has not been well evaluated. This information is critical for further improving the design of the E-peroxone process toward more effective TOC elimination.

To this end, this study investigated TOC removal from oxalic acid (OA) solutions by ozonation, electrolysis, O_3-electrolysis, and E-peroxone treatment. OA is a common intermediate formed in ozonation of many organic pollutants, such as aromatics and natural organic matter (von Gunten, 2003; Vecitis et al., 2010; Panizza and Cerisola, 2009; Brillas et al., 2009; Li et al., 2014). It is essentially unreactive with molecular O_3 ($k_{O3} \leq 0.04\ M^{-1}\ s^{-1}$ (Hoigné and Bader, 1983)), but reacts much faster with •OH ($k_{\cdot OH} = 1.4 \times 10^6\ M^{-1}\ s^{-1}$ (Buxton et al., 1988)) directly to CO_2 and H_2O (Pines and Reckhow, 2002). In addition, OA has high solubility in water and does not volatilize during gas sparging. These characteristics of OA facilitate the evaluation of TOC elimination due to •OH oxidation during the E-peroxone process. The kinetics of TOC elimination in the ozonation, electrolysis, O_3-electrolysis, and E-peroxone processes were analyzed to evaluate the respective contribution of the different •OH generation mechanisms for TOC elimination in the E-peroxone process. The effects of electrodes, current, and ozone concentration on TOC elimination were evaluated systematically for the E-peroxone process.

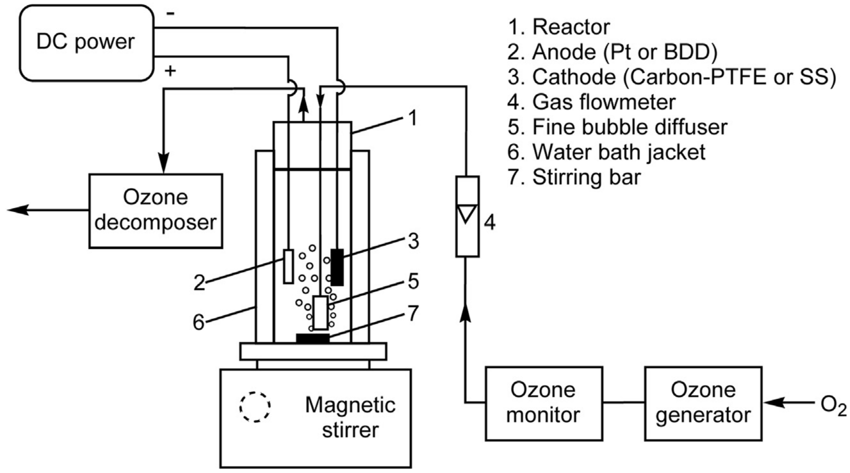

Fig. 1. Schematic of the reactor used for ozonation, electrolysis, O_3-electrolysis, and E-peroxone treatment of oxalic acid solutions.

2. Materials and methods

2.1. Chemicals and reagents

Anhydrous oxalic acid (99.99%), H_2O_2 (30 wt% solution), and potassium indigo trisulfonate (80–85%) were purchased from Sigma–Aldrich. Potassium titanium (IV) oxalate and other chemicals (e.g., Na_2SO_4, NaOH, and H_2SO_4) were analytical grade and purchased from Beijing Chemical Works Co., China. All solutions were prepared with ultrapure water (resistivity >18 MΩ).

2.2. Ozonation, electrolysis, O_3-electrolysis, and E-peroxone treatment of OA solution

Ozonation, electrolysis, O_3-electrolysis, and E-peroxone treatment of 400 mL OA solution (initial concentration of 180 mg/L) were conducted in an undivided acrylic column reactor (see Fig. 1). For ozonation treatment, an ozone generator (Tonglin Technology Co., China) was used to produce O_3 from high-purity O_2 gas (99.9%). The O_3 concentration in the ozone generator effluent (O_2 and O_3 gas mixture) can be adjusted by changing the ozone generator power. The ozone generator effluent was then sparged into the reactor at a constant flow rate of 0.4 L/min using a fine bubble diffuser. The electrolysis, O_3-electrolysis, and E-peroxone treatment were conducted under galvanostatic conditions using a DC power supply. The anode was either a platinum (Pt) sheet or a BDD thin-film electrode purchased from Adamant Technologies (Swiss). The cathode was a stainless steel (SS) plate for the electrolysis and O_3-electrolysis process and a carbon-PTFE electrode for the E-peroxone process. The carbon-PTFE electrode was prepared with Vulcan XC-72 carbon powder (Cabot Corp., USA), PTFE dispersion, and anhydrous alcohol (Wang et al., 2012). All the electrodes had an exposed area of 20 cm^2; this was with the exception of BDD electrode, which had an area of 12.5 cm^2. Before the BDD electrode was used, it was preconditioned in the blank electrolyte solution (0.05 M Na_2SO_4) at a current density of 20 mA/cm^2 for 10 min to prevent the accumulation of adsorbed organic compounds on the electrode surface. The distance between the anode and cathode was 2 cm. The supporting electrolyte was a 0.05 M Na_2SO_4 solution. For electrolysis alone, the treatment was initiated by turning on the DC power supply while the ozone generator was off. For O_3-electrolysis and E-peroxone treatment, the DC power supply and the ozone generator were turned on simultaneously. At applied currents of 100–500 mA, the average cell voltages were 3.9–9.0 V and 6.1–11.4 V for experiments conducted with the Pt and BDD anode, respectively. The ozone generator effluent was bubbled into the reactor at the same flow rate as in ozonation (0.4 L/min). In all experiments, the reactor was placed in a water bath (20 ± 1 °C), and the OA solution was thoroughly agitated with a magnetic stirring bar to achieve a homogeneous solution.

2.3. Analytical methods

The O_3 concentration in the sparged gas was monitored using an ozone analyzer (UV-300, Sumsun EP Hi-Tech Co., Beijing). During OA treatment, an aliquot of solution sample was collected from the reactor at preset time intervals. The concentration of dissolved ozone in the solution was determined with the indigo method (Bader and Hoigne, 1981). The H_2O_2 concentration was measured using potassium titanium (IV) oxalate method (Sellers, 1980), whereby H_2SO_4 solution (3 M) was used to adjust the sample pH to ~0 to prevent the interference of O_3 with H_2O_2 measurement (Milan-Segovia et al., 2007; Tong et al., 2011). OA concentration was measured using an HPLC-UV (Waters, USA) with an Atlantics column T (3.5 μm, 4.6 × 150 mm, Waters) at 210 nm (Wang et al., 2015). TOC was measured using a TOC-VCPH analyzer (Shimadzu Co. Japan).

3. Results and discussion

3.1. Electro-generation of H_2O_2 from O_2 at the carbon-PTFE cathode

The electro-generation of H_2O_2 from O_2 was evaluated by sparging pure O_2 into a 0.05 M Na_2SO_4 solution during electrolysis using the carbon-PTFE cathode. Fig. 2 shows that for a given applied current, H_2O_2 concentration increased almost linearly with reaction time. In addition, within the tested current range (100–500 mA), H_2O_2 concentration accumulated in the solution (1 h) also increased linearly with the current ($R^2 = 0.997$). This trend indicates that the rate of H_2O_2 generation is not limited by the mass transfer O_2 to the cathode, but by the applied current. The apparent current efficiency for H_2O_2 generation, which was calculated according to Eq. (14), was generally within 86.9–95.9% (see Fig. 2 inset). This result indicates that H_2O_2 can be efficiently electro-generated from sparged O_2 with high current efficiencies at the carbon-PTFE cathode, and the generation rate can be easily controlled by the applied current.

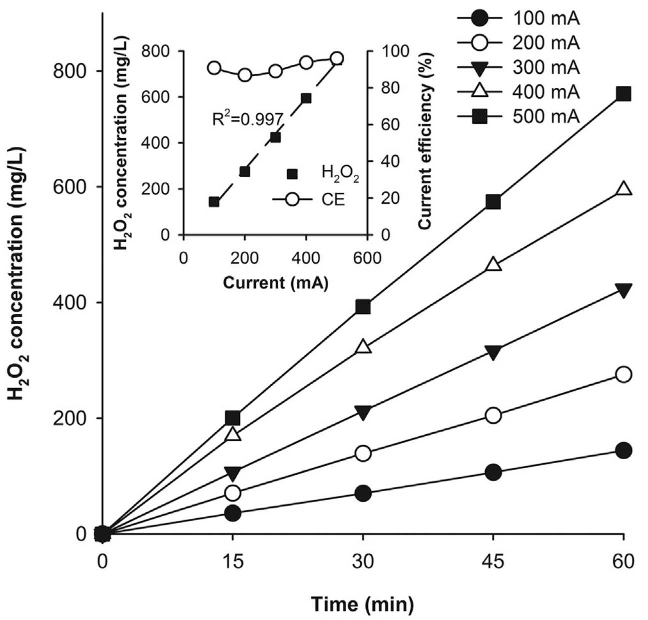

Fig. 2. Electro-generation of H_2O_2 from sparged O_2 at the carbon-PTFE cathode (400 mL of 0.05 M Na_2SO_4 solution; O_2 gas flow rate of 0.4 L/min; 20 cm^2 carbon-PTFE cathode; 2 cm^2 Pt anode). The inset plot shows the concentration of H_2O_2 at 1 h and the current efficiency (CE) of H_2O_2 production as a function of the applied current.

$$CE(\%) = \frac{nFC_{H_2O_2}V}{\int_0^t Idt} \times 100 \quad (14)$$

where n is the number of electrons consumed for converting O_2 to H_2O_2 (2 electrons), F is the Faraday constant (96,486 C/mol), C_{H2O2} is the concentration of H_2O_2 produced (mol/L), V is the solution volume (L), I is the current (A), and t is the electrolysis time (s).

3.2. Comparison of ozonation, electrolysis, O_3-electrolysis, and electro-peroxone process

TOC elimination from OA solutions by ozonation, electrolysis with the Pt anode and SS cathode (Pt/SS), O_3-electrolysis (Pt/SS), and E-peroxone (Pt/carbon-PTFE) process are compared in Fig. 3. The OA solution had an initial pH of 3, whereby OA is present predominantly as $HC_2O_4^-$ (accounting for ~93% of the total OA (Vecitis et al., 2010)). Similar to oxalic acid, $HC_2O_4^-$ reacts with O_3 very slowly ($k_{O3} = 5 \times 10^{-4}\ M^{-1}\ s^{-1}$) (Vecitis et al., 2010), but much faster with •OH ($k_{•OH} = 3.2 \times 10^7\ M^{-1}\ s^{-1}$) (Buxton et al., 1988). As Fig. 4(a) shows, the solution pH was quite stable during the ozonation treatment. Oxidation of OA by •OH formed from O_3 decomposition with OH^-, which occurs primarily at basic pH, is thus negligible in the ozonation treatment. Consequently, TOC was hardly removed by ozonation alone (Fig. 3). In comparison, electrolysis with the Pt anode and SS cathode removed 34.6% TOC after 2 h. This result agrees with the previous finding that OA can be electrochemically mineralized at Pt anodes during electrolysis (Martinez-Huitle et al., 2004). However, the mineralization current efficiency (MCE, calculated according to Eq. (15) (Garcia-Segura and Brillas, 2011)) was just 1.9% during the electrolysis process. This low MCE value indicates that OA mineralization is kinetically limited by its mass transfer to the Pt anode, and significant amounts of electricity are wasted in side reactions such as O_2 evolution during the electrolysis process.

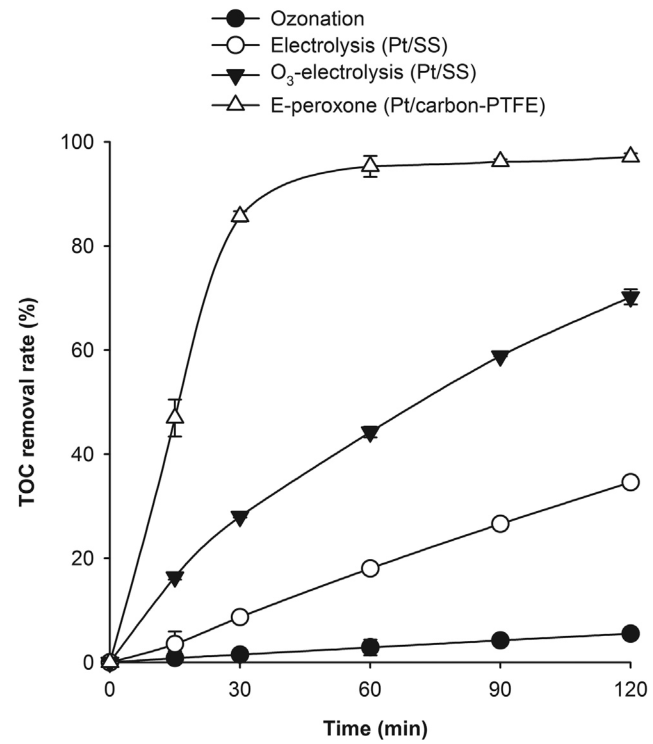

Fig. 3. TOC elimination by ozonation, electrolysis (Pt anode and SS cathode), O_3-electrolysis (Pt anode and SS cathode), and E-peroxone (Pt anode and carbon-PTFE cathode) processes (initial OA concentration = 2 mM; volume = 400 mL; sparging gas flow rate = 0.4 L/min; inlet O_3 gas phase concentration = 100 mg/L; current = 400 mA; average cell voltage = 7.8 V).

$$MCE(\%) = \frac{nFV_s\Delta(TOC)_{exp}}{4.32 \times 10^7 mlt} \times 100 \quad (15)$$

where n is the number of electrons consumed for mineralization of oxalic acid (2 electrons), F is the Faraday constant, V_s is the solution volume (L), Δ is the experimental TOC removal (mg/L), 4.32×10^7 is an homogenization factor (3600 s/h × 12,000 mg/mol), m is the number of carbon atoms of oxalic acid (2C atoms), I is the current (A), and t is the electrolysis time (h).

Notably, TOC removal was significantly enhanced when ozonation and electrolysis were combined together (see Fig. 3). For the O_3-electrolysis process that used the Pt anode and SS cathode, TOC removal reached 70.2% at 2 h. Adapting the O_3-electrolysis process to E-peroxone process (i.e., changing the cathode from SS to carbon-PTFE) further significantly increased TOC elimination yield, which reached 95.3% after 1 h of the E-peroxone treatment (Fig. 3).

The above results agree with the previous finding that ozonation and electrolysis can have significant synergistic effects for TOC elimination when they are coupled together, especially, in the form of E-peroxone process (Yuan et al., 2013; Bakheet et al., 2013). To get more insight into the synergy, we monitored the evolution profiles of aqueous O_3 and H_2O_2 during the different processes (see Fig. 4). For ozonation alone, the aqueous O_3 concentration increased rapidly to a pseudo-steady level (~30 mg/L) in equilibrium with its gas phase concentration (~100 mg/L) in the sparged gas (Fig. 4(b)). In comparison, the aqueous O_3 concentration fluctuated slightly at lower levels (~23 ± 3 mg/L) during the O_3-electrolysis process. This difference can be attributed to the consumption of dissolved O_3 in the O_3-electrolysis process, e.g., electro-reduction of O_3 at the cathode and O_3 decomposition with OH^- near the cathode (Kishimoto et al., 2008). These reactions transforms O_3 to •OH, and

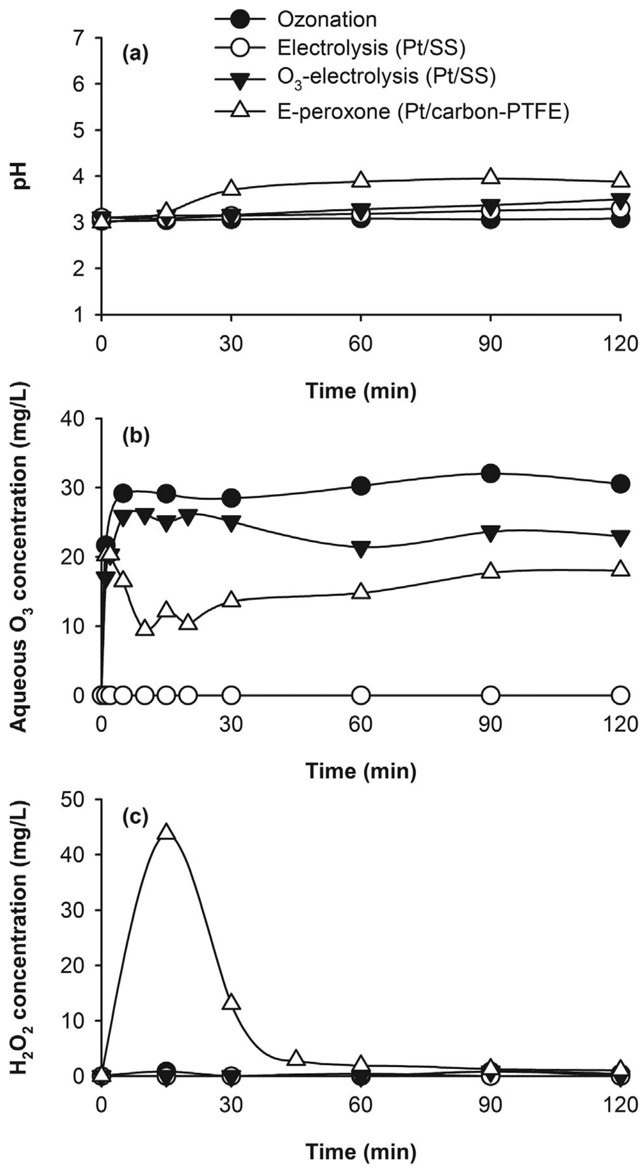

Fig. 4. Profiles of (a) pH, (b) aqueous O_3, and (c) H_2O_2 during ozonation, electrolysis (Pt anode and SS cathode), O_3-electrolysis (Pt anode and SS cathode), and E-peroxone (Pt anode and carbon-PTFE cathode) processes (initial OA concentration = 2 mM; volume = 400 mL; sparging gas flow rate = 0.4 L/min; inlet O_3 gas phase concentration = 100 mg/L; current = 400 mA; average cell voltage = 7.8 V).

can thus enhance OA oxidation in the O_3-electrolysis process (see Fig. 3) (Qiu et al., 2014; Kishimoto et al., 2007, 2008).

Adapting the O_3-electrolysis to E-peroxone process (i.e., changing the cathode from SS to carbon-PTFE) further considerably decreased aqueous O_3 concentration (Fig. 4(b)). This result indicates that aqueous O_3 is more rapidly consumed in the E-peroxone process than in the O_3-electrolysis process. As aforementioned, SS and other metal (e.g., Cu and Ti) electrodes cannot produce H_2O_2 from O_2 (Sudoh et al., 1985; Li et al., 2013), whereas carbon-based electrodes can effectively convert O_2 to H_2O_2 (see Fig. 2). The in-situ generated H_2O_2 then diffuses into the bulk solution and reacts with O_3 to yield •OH. Thus, in addition to being transformed to •OH via reactions such as O_3 electro-reduction and O_3 decomposition with OH^- at the cathode in the O_3-electrolysis process, extra O_3 can be transformed to •OH via the electrochemically driven peroxone reaction in the E-peroxone process. Consequently, both O_3 consumption and TOC elimination were considerably increased by adapting the O_3-electrolysis process to the E-peroxone process.

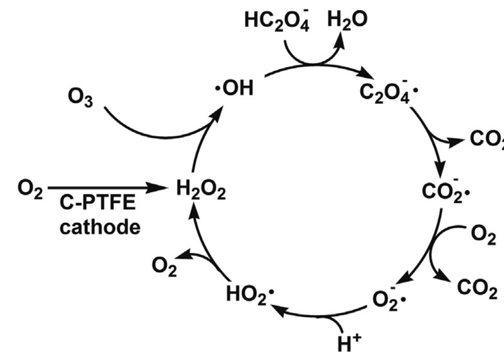

Fig. 5. Schematic of radical–chain reactions that regenerate H_2O_2 during bioxalate oxidation in the E-peroxone process.

The evolution of H_2O_2 during the four different processes is compared in Fig. 4(c). Virtually no H_2O_2 was detected during the ozonation, electrolysis (Pt/SS), and O_3-electrolysis (Pt/SS) processes. In contrast, high concentrations of H_2O_2 (up to 43.7 mg/L) were detected at the early stage (15–30 min) of the E-peroxone process. During the same period, TOC was also rapidly removed from the OA solution (see Fig. 3). These results confirm that when carbon-PTFE electrode is used as the cathode, considerable amounts of H_2O_2 can be generated in the E-peroxone process, and thus significantly enhance O_3 transformation to •OH for pollutant degradation.

Interestingly, the concentration of H_2O_2 increased rapidly in the first 15 min of the E-peroxone process, and then decreased considerably with further increase of the reaction time (Fig. 4(c)). This trend indicates that H_2O_2 was produced more rapidly than it was consumed at the early stage of E-peroxone treatment, whereas it was consumed more rapidly than it was produced after 15 min. This change can be possibly explained as follows.

In the E-peroxone process, H_2O_2 is produced stably from O_2 at the carbon-PTFE cathode (see Fig. 2), and then consumed mainly in the reaction with O_3 to yield •OH (H_2O_2 itself does not react actively with OA (Vecitis et al., 2010)). However, the reaction of •OH with OA can initiate a series of radical–chain reactions (Eqs. (16)–(19)) through which H_2O_2 is regenerated during OA oxidation to CO_2 (Vecitis et al., 2010; Martinez-Huitle et al., 2004; Garcia-Segura and Brillas, 2011). The regenerated H_2O_2, together with the electro-generated H_2O_2, can then further react with O_3 to yield •OH, thus multiplying the chain-reaction loop shown in Fig. 5. As shown, the chain reactions are initiated by the reaction of OA with •OH. The rate of H_2O_2 regeneration is thus expected to be proportional to the OA concentration in the solution. This may explain why H_2O_2 is produced more rapidly (from both electro-generation and chain-reaction regeneration) than it is consumed at the early stage of E-peroxone process when OA concentration is still high. However, as OA is rapidly removed from the solution, the rate of H_2O_2 regeneration decreases considerably. This led to the decrease of H_2O_2 concentration as the E-peroxone process proceeded. Finally, H_2O_2 regeneration via the chain-reaction loop stops after OA is completely eliminated from the solution. Only insignificant amount of H_2O_2 was detected at the late stage (60–120 min) of the E-peroxone process (Fig. 4(c)), suggesting that the electro-generated H_2O_2 is almost completely consumed in the reaction with O_3.

$$HC_2O_4^- + \cdot OH \rightarrow C_2O_4^- \cdot + H_2O \quad (16)$$

$$C_2O_4^{-}\cdot \rightarrow CO_2^{-}\cdot + CO_2 \quad (17)$$

$$CO_2^{-}\cdot + O_2 \rightarrow O_2^{-}\cdot + CO_2 \quad (18)$$

$$2O_2^{-}\cdot + 2H^{+} \rightarrow H_2O_2 + O_2 \quad (19)$$

It should be pointed out that similar chain-reaction loop for H_2O_2 regeneration has also been suggested during OA oxidation by other AOPs (e.g., electro-Fenton and sonozone (combined process of ultrasonic and O_3)), and considered an important mechanism for enhanced TOC elimination in these processes (Vecitis et al., 2010; Garcia-Segura and Brillas, 2011). However, this chain-reaction loop is unlikely to occur at typical pH values (~6–8) of water treatment, whereby $HO_2\cdot/O_2^{-}\cdot$ (pKa = 4.8) exists mainly as $O_2^{-}\cdot$ (Bielski et al., 1985). At typical pH range of water treatment, the reaction of $O_2^{-}\cdot$ with H^{+} to $HO_2\cdot$ is therefore unfavorable, and $O_2^{-}\cdot$ would be more likely scavenged rapidly by O_3 (Eq. (6), $k = 1.6 \times 10^9\ M^{-1}\ s^{-1}$ (von Gunten, 2003)).

3.3. Effect of anode type on TOC elimination

The above results indicate that the type of cathode (SS or carbon-PTFE) can play a critical role in TOC removal in combined processes of ozonation and electrolysis (O_3-electrolysis or E-peroxone). To investigate the role of anode in TOC elimination, we replaced the Pt anode with a BDD anode and repeated the above tests. Because BDD has a greater O_2-overpotential than Pt (Panizza and Cerisola, 2009), the average cell voltage increased from ~7.8 V to ~10.2 V (current = 400 mA) when the Pt anode was replaced by the BDD anode. The result shows that TOC was removed at comparable rates when either Pt or BDD was used as the anode in the electrolysis and E-peroxone processes (see Figs. 3 and 6). However, for the O_3-electrolysis process, TOC was removed much more rapidly when BDD was used as the anode (97.6% at 2 h) than when Pt was used (70.2% at 2 h). This result suggests that the type of anode can also have complicated influence on TOC elimination in combined processes of ozonation and electrolysis.

Unlike Pt anodes, which are inefficient at producing •OH from water discharge, BDD anodes are well-known for their high activity for •OH generation when electrolysis is operated at anodic potentials higher that for oxygen evolution (2.3 V vs. SHE for BDD) (Panizza and Cerisola, 2009; Bejan et al., 2012). Therefore, OA is oxidized via distinct mechanisms in electrolysis that uses Pt or BDD anode (Martinez-Huitle et al., 2004; Garcia-Segura and Brillas, 2011; Scialdone et al., 2008). When Pt is used as the anode, OA is mainly oxidized via direct electron transfer after it has been adsorbed onto the anode surface (Eq. (20) and (21)). In contrast, OA is mainly oxidized by •OH produced from water oxidation when BDD is used as the anode (Eqs. 16–18) (Martinez-Huitle et al., 2004; Garcia-Segura and Brillas, 2011; Scialdone et al., 2008). Despite the different reaction mechanisms, previous studies have indicated that OA can be effectively oxidized by electrolysis using either Pt or BDD anode (Martinez-Huitle et al., 2004). Consistently, the present study shows that OA was oxidized at similar rates in the electrolysis process using the Pt or BDD anode (Figs. 3 and 6).

$$HC_2O_4^{-} \rightarrow HC_2O_{4(ads)}^{-} \quad (20)$$

$$HC_2O_{4(ads)}^{-} \rightarrow 2CO_2 + H^{+} + 2e^{-} \quad (21)$$

However, using BDD as the anode in the O_3-electrolysis process resulted in much higher TOC elimination yield (97.6% at 2 h) than using Pt as the anode (70.2% at 2 h). This difference can be probably attributed to the fact that BDD anode is effective at producing •OH from water discharge, whereas Pt anode is not. Previous studies have indicated that some •OH generated at the BDD anode would undergo recombination to form H_2O_2 (Panizza and Cerisola, 2009). Indeed, we found that small amounts of H_2O_2 (4.1 mg/L at 2 h) accumulated in the solution when BDD was used as the anode in electrolysis alone. In contrast, no H_2O_2 accumulation was observed for the electrolysis process using the Pt anode (see Fig. 4(c)). In electrolysis alone, the BDD anode-induced H_2O_2 would not contribute much to TOC removal because H_2O_2 reacts with OA very slowly ($k < 0.2\ M^{-1}\ s^{-1}$ (Vecitis et al., 2010)). However, it can react with sparged O_3 to yield •OH, thus enhancing OA oxidation in the O_3-electrolysis process. This explains why using the BDD anode resulted in more rapid TOC elimination than using the Pt anode in the O_3-electrolysis process (see Figs. 3 and 6).

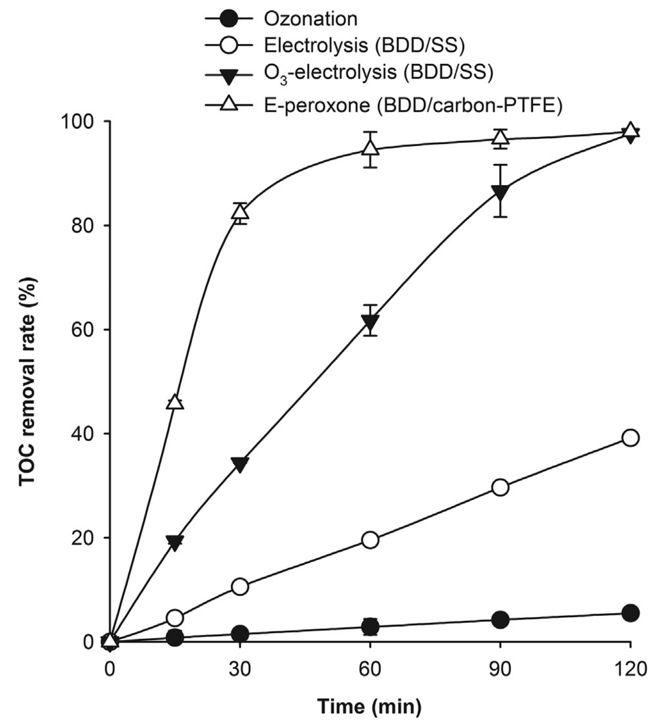

Fig. 6. TOC elimination by ozonation, electrolysis (BDD anode and SS cathode), O_3-electrolysis (BDD anode and SS cathode), and E-peroxone (BDD anode and carbon-PTFE cathode) processes (initial OA concentration = 2 mM; volume = 400 mL; sparging gas flow rate = 0.4 L/min; inlet O_3 gas phase concentration = 100 mg/L; current = 400 mA; average cell voltage = 10.2 V).

Unlike in the O_3-electrolysis process, the type of anode had little influence on TOC elimination rates in the E-peroxone process. As shown in Figs. 3 and 6, TOC was actually removed at almost the same rate when either Pt or BDD was used as the anode in the E-peroxone process. This result is possibly because as H_2O_2 is generated from O_2 much more rapidly at the carbon-PTFE cathode (Fig. 2), the contribution of BDD anode for H_2O_2 generation is negligible in the E-peroxone process.

3.4. Evaluation of the synergy for TOC elimination in the E-peroxone process

Kinetic analysis shows that TOC elimination follows pseudo-first-order kinetics in all processes, i.e., ozonation, electrolysis, O_3-electrolysis, and E-peroxone process (see Table 1). Notably, the apparent rate constants of TOC elimination (k_{app}) in the O_3-electrolysis and E-peroxone processes are significantly higher than the linear addition of the individual rates of corresponding ozonation

Table 1
Pseudo-first-order rate constants and square regression coefficient for mineralization of oxalic acid in different processes.

Process	Anode	Cathode	$K_{overall} \times 10^3$ (min^{-1})	r^2	Enhancement (%)
Ozonation	–	–	0.48	0.999	–
Electrolysis	Pt	SS	3.45	0.996	–
Electrolysis	BDD	SS	3.98	0.994	–
O_3-electrolysis	Pt	SS	10.02	0.998	155
O_3-electrolysis	BDD	SS	15.55	0.994	249
E-peroxone	Pt	Carbon-PTFE	53.10	0.970	1252
E-peroxone	BDD	Carbon-PTFE	49.76	0.984	1016

and electrolysis processes. This result confirms that when ozonation and electrolysis are combined together (O_3-electrolysis and E-peroxone), they have significant synergistic effects for TOC elimination.

In previous studies, this synergy has been mainly attributed to the production of •OH from several mechanisms in the E-peroxone process, e.g., cathodic reduction of O_3, O_3 decomposition near the cathode, and O_3 reaction with H_2O_2 electro-generated at the carbon-PTFE cathode (Yuan et al., 2013; Bakheet et al., 2013). In addition, the present study shows that when BDD is used as the anode, it can also produce small amounts of H_2O_2 from the self-termination reaction of BDD(•OH). The anode-induced H_2O_2 can also react with O_3 to yield •OH, and thus enhance TOC elimination (this effect is quite pronounced in the O_3-electrolysis process, but is negligible in the E-peroxone process, see discussion of Fig. 6).

To evaluate the respective contribution of the above mechanisms for TOC elimination, an approach similar to that proposed by Hoffmann's group (Vecitis et al., 2010; Weavers et al., 1998; Lesko et al., 2006) for sonozone process was taken to analyze the kinetics of TOC abatement in the O_3-electrolysis and E-peroxone processes. As shown in Eq. (22), the overall removal rate of OA in the combined processes of ozonation and electrolysis can be described by a linear combination of contributing terms.

$$-\frac{dC}{dt} = k_{O_3}[C] + k_E[C] + k_{O_3/E}[C] \tag{22}$$

where k_{O3}, k_E, and $k_{O3/E}$ are the pseudo-first-order rate constants of TOC elimination for ozonation, electrolysis, and the synergistic kinetic effect upon combining the two systems (O_3-electrolysis or E-peroxone), respectively.

When the terms are combined, Eq. (23) can be expressed as

$$-\frac{dC}{dt} = \left(k_{O_3} + k_E + k_{O_3/E}\right)[C] = k_{overall}[C] \tag{23}$$

where $k_{overall}$ is the overall pseudo-first reaction rate constant in the O_3-electrolysis and E-peroxone processes (i.e., those listed in Table 1).

The enhancement of OA elimination in O_3-electrolysis and E-peroxone processes is then calculated according to Eq. (24) (Weavers et al., 1998).

$$\text{Enhancement (\%)} = \frac{k_{O_3/E}}{k_{O_3} + k_E} \times 100 \tag{24}$$

The calculations show that O_3-electrolysis using the Pt anode and SS cathode enhanced the rate of OA elimination by 155% (Table 1), which can be mainly attributed to the electro-reduction of O_3 to •OH at the SS cathode and O_3 decomposition to •OH near the cathode (Kishimoto et al., 2005). Using BDD as the anode in O_3-electrolysis further increased the enhancement factor to 249%, probably due to the formation of small amounts of H_2O_2 at the BDD anode. Notably, by simply replacing the SS cathode with the carbon-PTFE cathode to electrochemically generate H_2O_2 from O_2 (i.e., adapting O_3-electrolysis for E-peroxone), the enhancement factor increased dramatically to 1252 and 1016% for the E-peroxone with the Pt and BDD anode, respectively.

The kinetic analysis confirms that electro-generation of H_2O_2 at the carbon-PTFE cathode and its subsequent reaction with sparged O_3 to produce •OH are the most important mechanism for the enhanced pollutant degradation in the E-peroxone process. In comparison, O_3 reduction at the cathode, O_3 decomposition to •OH near the cathode, and H_2O_2 generation at the BDD anode contribute much less to the enhancement. Indeed, because O_3 has a low solubility in water, the rate of electro-reduction of O_3 to •OH is often kinetically limited by the mass transfer of O_3 to the cathode (Kishimoto et al., 2005; Bakheet et al., 2013)). Moreover, O_3 reacts only slowly with OH^- ($k = 70\ M^{-1}\ s^{-1}$ (von Gunten, 2003)). Consequently, cathodic reduction of O_3 to •OH and O_3 decomposition with OH^- to •OH enhanced TOC elimination just moderately (e.g., enhancement factor of 155–249% for the O_3-electrolysis process using the SS cathode).

In comparison, Fig. 2 shows that H_2O_2 can be produced efficiently at the carbon-PTFE cathode (e.g., current efficiencies of 86.9–95.9%), and no mass transfer limitation of O_2 on H_2O_2 electro-generation was observed within the tested current range (100–500 mA). More importantly, H_2O_2 has much longer life time than •OH. The electro-generated H_2O_2 can therefore diffuse out of the cathodic diffusion layer to react with O_3 in the bulk solution. Consequently, considerable amounts of •OH can be generated to oxidize pollutants rapidly in the bulk solution. This circumvents the intrinsic limitation of electrolysis for pollutant degradation, i.e., the

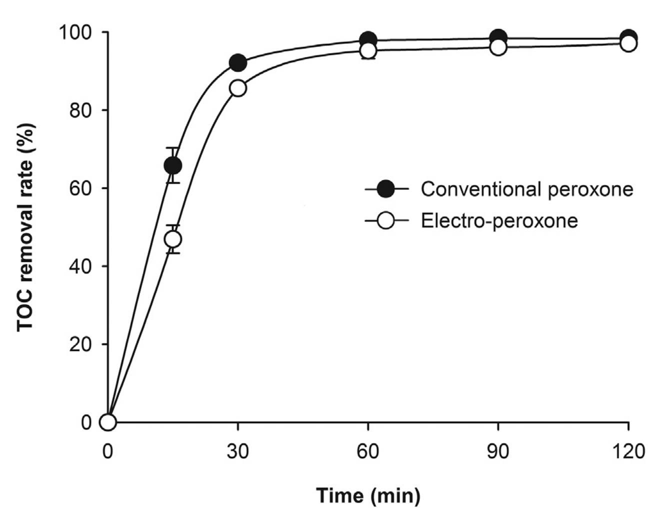

Fig. 7. Comparison of TOC removal by conventional peroxone and electro-peroxone processes (initial OA concentration = 2 mM; volume = 400 mL; sparging gas flow rate = 0.4 L/min; inlet O_3 gas phase concentration = 100 mg/L; 20 cm^2 carbon-PTFE cathode; 20 cm^2 Pt anode; current = 400 mA for electro-peroxone; average cell voltage = 7.8 V; addition of 480 mg H_2O_2 for conventional peroxone process).

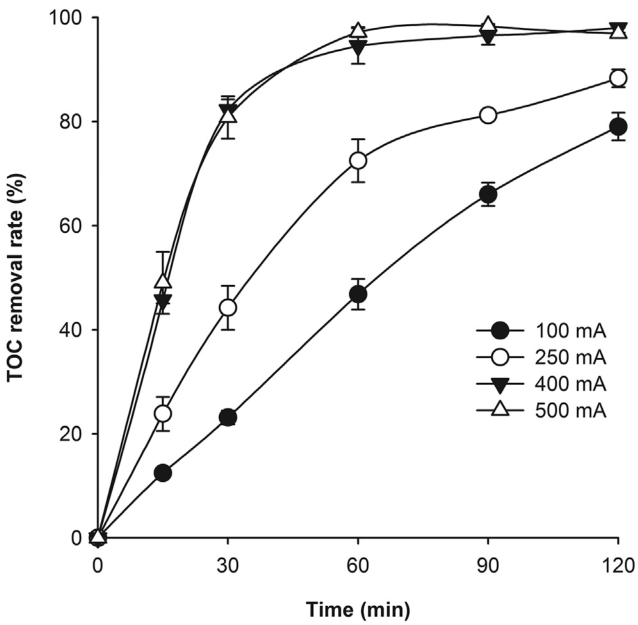

Fig. 8. Effects of applied current on TOC elimination in the E-peroxone process (initial OA concentration = 2 mM; volume = 400 mL; 20 cm^2 carbon-PTFE cathode; 12.5 cm^2 BDD anode; sparging gas flow rate = 0.4 L/min; inlet O_3 gas phase concentration = 100 mg/L).

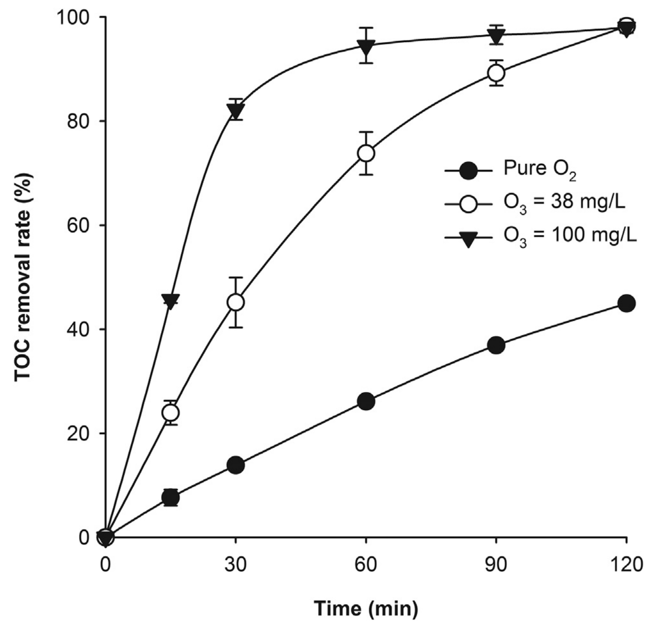

Fig. 9. Effects of ozone concentration on TOC elimination in the E-peroxone process (initial OA concentration = 2 mM; volume = 400 mL; 20 cm^2 carbon-PTFE cathode; 12.5 cm^2 BDD anode; sparging gas flow rate = 0.4 L/min; current = 400 mA; average cell voltage = 10.2 V).

degradation kinetics of pollutants is limited by their mass transfer to the anode (Yuan et al., 2013; Li et al., 2014). Therefore, the E-peroxone process can eliminate TOC from water much more rapidly than ozonation, electrolysis, and O_3-electrolysis processes.

3.5. Comparison with conventional peroxone process

Fig. 7 shows TOC removal from OA solutions by the E-peroxone and conventional peroxone process, in which H_2O_2 was externally added. Based on the result reported in Fig. 2, approximately 480 mg of H_2O_2 can be electro-generated during 2 h of the E-peroxone process operated at 400 mA. The same amount of H_2O_2 was therefore added in the conventional peroxone process. To minimize the side reaction of H_2O_2 with •OH (Eq. (25)), which may occur to some extent at high H_2O_2 concentrations (Vecitis et al., 2010; Li et al., 2013), one-eighth of the total H_2O_2 dose (480 mg) was stepwise added into the OA solution every 15 min during the 2 h of conventional peroxone process (e.g., add ~60 mg H_2O_2 at 0, 15, and 30 min, respectively).

$$H_2O_2 + \cdot OH \rightarrow HO_2\cdot + H_2O \quad (25)$$

As shown in Fig. 7, TOC was removed from OA solution more rapidly by conventional peroxone process than the E-peroxone process during the first 30 min. This difference can be mainly attributed to the different way of H_2O_2 supplying in the two processes. For the conventional peroxone process, approximately 60 mg H_2O_2 was added into OA solution at 0 min, whereas it took 15 min for the E-peroxone process to generate the same amount of H_2O_2 in the solution. Therefore, it is assumable that the "startup" of the peroxone reaction (and chain-reaction loop for H_2O_2 regeneration) would be more intense in the conventional peroxone process than in the E-peroxone process, leading to more rapid TOC removal at the initial stage of conventional peroxone process. However, similar TOC removal efficiency was obtained for the two processes after 1 h treatment (Fig. 7) when considerable amount of H_2O_2 had been continuously electro-generated in the E-peroxone process.

The above comparison suggests that the E-peroxone process may provide a comparably effective way to degrade pollutants as conventional peroxone process. Meanwhile, the electro-generation of H_2O_2 eliminates the potential risks associated with the transportation, storage, and use of high concentration H_2O_2 solutions in conventional peroxone process. Furthermore, when BDD is used as the anode, the E-peroxone process can anodically oxidize refractory Fe^{3+}-oxalate complexes that resist oxidation by aqueous •OH, hence improving TOC removal from wastewater that contains Fe^{3+} ions (see SD for more detail). Compared with conventional peroxone process, the E-peroxone process may thus offer a safer and more convenient alternative for water and wastewater treatment.

3.6. Effects of applied current on TOC elimination in E-peroxone

Fig. 8 shows that as the applied current was increased from 100 to 400 mA (average cell voltage increased from 6.1 to 10.2 V), TOC was more rapidly eliminated from OA solutions. Nevertheless, further increasing the current to 500 mA (average cell voltage = 11.4 V) did not increase TOC elimination yet further. Similar trends have been observed in our previous E-peroxone studies (Yuan et al., 2013; Bakheet et al., 2013). As Fig. 2 shows, the rate of H_2O_2 production is proportional to the applied current within the tested current range (100–500 mA). It was therefore anticipated that increasing the current would produce more H_2O_2 to react with O_3, hence yielding more •OH to enhance TOC elimination. However, our previous studies have found that under similar reaction conditions (e.g., reactor configuration, O_3 dosage, and electrodes), the •OH generation rate would become limited by the mass transfer of O_3 from the gas phase to liquid when the current is increased beyond 400 mA (Yuan et al., 2013; Bakheet et al., 2013). When there is insufficient aqueous O_3 to react with electro-generated H_2O_2, the excess H_2O_2 contributes less to TOC elimination since it reacts only slowly with OA ($k < 0.2\ M^{-1}\ s^{-1}$ (Vecitis et al., 2010)). Therefore, TOC elimination kinetics increased as the current was increased from 100 to 400 mA, but did not further increase by further increasing the applied current.

3.7. Effects of O_3 concentration on TOC elimination in E-peroxone

As the O_3 concentration in the sparged gas was increased, TOC was removed from OA solutions more rapidly (Fig. 9). This can be easily rationalized because increasing the O_3 concentration in the sparged gas enhances the mass transfer of O_3 from the gas phase to the liquid. Consequently, more •OH can be generated from reactions such as O_3 reaction with H_2O_2 and O_3 cathodic reduction, resulting in enhanced TOC elimination in the E-peroxone process. Note that sparging pure O_2 (i.e., $O_3 = 0$ mg/L) during electrolysis using the carbon-PTFE cathode can produce significant amount of H_2O_2 in the solution (~600 mg/L at 400 mA, see Fig. 2). Sparging pure O_2 thus enhanced TOC elimination slightly (44.9%) compared with electrolysis alone (39.2%) (see Fig. 6), although the reaction of H_2O_2 with OA is slow ($k < 0.2\ M^{-1}\ s^{-1}$ (Vecitis et al., 2010)).

The results of this study show that the E-peroxone process can considerably enhance TOC removal from OA solutions as compared to ozonation, electrolysis, and O_3-electrolysis processes. This enhancement is mainly because significant amounts of •OH can be generated from electrochemically induced reactions such as O_3 with electro-generated H_2O_2 and O_3 electro-reduction at the cathode in the E-peroxone process. The electrochemically induced •OH can then oxidize ozone-refractory OA directly to CO_2 and H_2O. As a result, complete OA mineralization can be obtained by the E-peroxone process. However, it should be noted the present study was conducted under conditions that are different from typical conditions of water treatment. For example, all experiments were conducted in acidic OA solutions (pH ~3) prepared with ultrapure water; these conditions were employed to prevent •OH formation from O_3 reactions with OH^- (although this reaction is very slow and possibly tolerable at pH ~7) and other matrix components (e.g., natural organic matter (NOM)) in the bulk solution (von Gunten, 2003; Pocostales et al., 2010), which would complicate the evaluation of the role of electrochemically induced •OH in the E-peroxone process. By contrast, typical water treatment involving ozone based processes is usually operated at pH of 6–9, and real water may contain some matrix components (e.g., NOM) that can react with O_3 to form •OH (von Sonntag and von Gunten, 2012; Pocostales et al., 2010). It is therefore expected that a distinctive oxidation of OA may occur under conditions of conventional ozonation. In addition, due to the small OA solution volume (400 mL) used in this study, much higher O_3 doses (e.g. ~100 mg/L gas phase) than typical conditions of water treatment were used to enhance O_3 mass transfer from the gas phase to liquid phase. Therefore, it is expected that complete mineralization of pollutants is unlikely to occur under typical conditions of water treatment, considering the presence of many side reactions with other water matrix components (e.g., NOM and carbonates) and the high energy demand to treat to such an extent. More research is needed to evaluate the performance and energy cost of the E-peroxone process for pollutant degradation under typical conditions of water treatment.

4. Conclusions

This study demonstrates that when conventional ozonation and electrolysis are combined in the E-peroxone process, they can achieve a significant synergy for TOC elimination from water. This synergy can be mainly attributed to several mechanisms that enhance O_3 transformation to •OH in the E-peroxone system, e.g., electro-generation of H_2O_2 from O_2 at the carbon-PTFE cathode and its subsequent peroxone reaction with O_3 to •OH, electro-reduction of O_3 to •OH at the cathode, and O_3 decomposition to •OH near the cathode. Among those, the electrochemically-driven peroxone reaction is the most important mechanism for the enhanced TOC elimination, while the other mechanisms contribute much less. Effective generation of H_2O_2 from O_2 at the cathode is thus the key to maximize TOC elimination in the E-peroxone process.

Acknowledgments

This research is supported by the National High Technology Research and Development of China (No. 2013AA06A305), the special fund of State Key Joint Laboratory of Environment Simulation and Pollution Control (13Y01ESPCT), Scholarship Award for Excellent Doctoral Student granted by Yunnan Province, Tsinghua University Initiative Scientific Research Program (20141081174), and Collaborative Innovation Center for Regional Environmental Quality.

Appendix A. Supplementary data

Supplementary data related to this article can be found at http://dx.doi.org/10.1016/j.watres.2015.05.024.

References

Bader, H., Hoigne, J., 1981. Determination of ozone in water by the indigo method. Water Res. 15 (4), 449–456.

Bakheet, B., Qiu, C., Yuan, S., Wang, Y., Yu, G., Deng, S., Huang, J., Wang, B., 2014. Inhibition of polymer formation in electrochemical degradation of p-nitrophenol by combining electrolysis with ozonation. Chem. Eng. J. 252, 17–21.

Bakheet, B., Yuan, S., Li, Z., Wang, H., Zuo, J., Komarneni, S., Wang, Y., 2013. Electro-peroxone treatment of orange II dye wastewater. Water Res. 47 (16), 6234–6243.

Bejan, D., Guinea, E., Bunce, N.J., 2012. On the nature of the hydroxyl radicals produced at boron-doped diamond and Ebonex® anodes. Electrochim. Acta 69, 275–281.

Bielski, B.H., Cabelli, D.E., Arudi, R.L., Ross, A.B., 1985. Reactivity of HO_2/O_2^- radicals in aqueous solution. J. Phys. Chem. Ref. Data 14 (4), 1041–1100.

Brillas, E., Sires, I., Oturan, M.A., 2009. Electro-fenton process and related electrochemical technologies based on Fenton's reaction chemistry. Chem. Rev. 109 (12), 6570–6631.

Buxton, G.V., Greenstock, C.L., Helman, W.P., Ross, A.B., 1988. Critical review of rate constants for reactions of hydrated electrons, hydrogen atoms and hydroxyl radicals ($OH/•O^-) in aqueous solution. J. Phys. Chem. Ref. Data 17 (2), 513–886.

Fischbacher, A., von Sonntag, J., von Sonntag, C., Schmidt, T.C., 2013. The $OH radical yield in the $H_2O_2 + O_3$ (peroxone) reaction. Environ. Sci. Technol. 47 (17), 9959–9964.

García-Morales, M.A., Roa-Morales, G., Barrera-Díaz, C., Bilyeu, B., Rodrigo, M.A., 2013. Synergy of electrochemical oxidation using boron-doped diamond (BDD) electrodes and ozone (O_3) in industrial wastewater treatment. Electrochem. Commun. 27, 34–37.

Garcia-Segura, S., Brillas, E., 2011. Mineralization of the recalcitrant oxalic and oxamic acids by electrochemical advanced oxidation processes using a boron-doped diamond anode. Water Res. 45 (9), 2975–2984.

Hoigné, J., Bader, H., 1983. Rate constants of reactions of ozone with organic and inorganic compounds in water—II: dissociating organic compounds. Water Res. 17 (2), 185–194.

Kishimoto, N., Morita, Y., Tsuno, H., Oomura, T., Mizutani, H., 2005. Advanced oxidation effect of ozonation combined with electrolysis. Water Res. 39 (19), 4661–4672.

Kishimoto, N., Nakagawa, T., Asano, M., Abe, M., Yamada, M., Ono, Y., 2008. Ozonation combined with electrolysis of 1,4-dioxane using a two-compartment electrolytic flow cell with solid electrolyte. Water Res. 42 (1–2), 379–385.

Kishimoto, N., Yasuda, Y., Mizutani, H., Ono, Y., 2007. Applicability of ozonation combined with electrolysis to 1,4-dioxane removal from wastewater containing radical scavengers. Ozone Sci. Eng. 29 (1), 13–22.

Lesko, T., Colussi, A.J., Hoffmann, M.R., 2006. Sonochemical decomposition of phenol: evidence for a synergistic effect of ozone and ultrasound for the elimination of total organic carbon from water. Environ. Sci. Technol. 40 (21), 6818–6823.

Li, X., Wang, Y., Yuan, S., Li, Z., Wang, B., Huang, J., Deng, S., Yu, G., 2014. Degradation of the anti-inflammatory drug ibuprofen by electro-peroxone process. Water Res. 63, 81–93.

Li, Z., Yuan, S., Qiu, C., Wang, Y., Pan, X., Wang, J., Wang, C., Zuo, J., 2013. Effective degradation of refractory organic pollutants in landfill leachate by electro-peroxone treatment. Electrochim. Acta 102, 174–182.

Martinez-Huitle, C.A., Ferro, S., De Battisti, A., 2004. Electrochemical incineration of oxalic acid: role of electrode material. Electrochim. Acta 49 (22–23),

4027–4034.
Merenyi, G., Lind, J., Naumov, S., von Sonntag, C., 2010a. The reaction of ozone with the hydroxide ion: mechanistic considerations based on thermokinetic and quantum chemical calculations and the role of HO_4^- in superoxide dismutation. Chem.-A Eur. J. 16 (4), 1372–1377.
Merenyi, G., Lind, J., Naumov, S., von Sonntag, C., 2010b. Reaction of ozone with hydrogen peroxide (peroxone process): a revision of current mechanistic concepts based on thermokinetic and quantum-chemical considerations. Environ. Sci. Technol. 44 (9), 3505–3507.
Milan-Segovia, N., Wang, Y.J., Cannon, F.S., Voigt, R.C., Furness, J.C., 2007. Comparison of hydroxyl radical generation for various advanced oxidation combinations as applied to foundries. Ozone Sci. Eng. 29 (6), 461–471.
Panizza, M., Cerisola, G., 2001. Removal of organic pollutants from industrial wastewater by electrogenerated Fenton's reagent. Water Res. 35 (16), 3987–3992.
Panizza, M., Cerisola, G., 2009. Direct and mediated anodic oxidation of organic pollutants. Chem. Rev. 109 (12), 6541–6569.
Petre, A.L., Carbajo, J.B., Rosal, R., Garcia-Calvo, E., Perdigon-Melon, J.A., 2013. CuO/SBA-15 catalyst for the catalytic ozonation of mesoxalic and oxalic acids. Water matrix effects. Chem. Eng. J. 225, 164–173.
Pines, D.S., Reckhow, D.A., 2002. Effect of dissolved cobalt(II) on the ozonation of oxalic acid. Environ. Sci. Technol. 36 (19), 4046–4051.
Pocostales, J.P., Sein, M.M., Knolle, W., von Sonntag, C., Schmidt, T.C., 2010. Degradation of ozone-refractory organic phosphates in wastewater by ozone and ozone/hydrogen peroxide (peroxone): the role of ozone consumption by dissolved organic matter. Environ. Sci. Technol. 44 (21), 8248–8253.
Qiu, C., Yuan, S., Li, X., Wang, H., Bakheet, B., Komarneni, S., Wang, Y., 2014. Investigation of the synergistic effects for p-nitrophenol mineralization by a combined process of ozonation and electrolysis using a boron-doped diamond anode. J. Hazard. Mater. 280, 644–653.
Scialdone, O., Galia, A., Guarisco, C., Randazzo, S., Filardo, G., 2008. Electrochemical incineration of oxalic acid at boron doped diamond anodes: role of operative parameters. Electrochim. Acta 53 (5), 2095–2108.
Sellers, R.M., 1980. Spectrophotometric determination of hydrogen peroxide using potassium titanium(IV) oxalate. Analyst 105 (1255), 950–954.
Sudoh, M., Kitaguchi, H., Koide, K., 1985. Electrochemical production of hydrogen peroxide by reduction of oxygen. J. Chem. Eng. Jpn. 18 (5), 409–414.
Tong, S.-P., Li, W.-W., Zhao, S.-Q., Ma, C.-A., 2011. Titanium (IV)-improved H_2O_2/O_3 process for acetic acid degradation under acid conditions. Ozone Sci. Eng. 33 (6), 441–448.
Vecitis, C.D., Lesko, T., Colussi, A.J., Hoffmann, M.R., 2010. Sonolytic decomposition of aqueous bioxalate in the presence of ozone. J. Phys. Chem. A 114 (14), 4968–4980.
von Gunten, U., 2003. Ozonation of drinking water: part I. Oxidation kinetics and product formation. Water Res. 37 (7), 1443–1467.
von Sonntag, C., von Gunten, U., 2012. Chemistry of Ozone in Water and Wastewater Treatment. IWA Publishing.
Wang, H., Bakheet, B., Yuan, S., Li, X., Yu, G., Murayama, S., Wang, Y., 2015. Kinetics and energy efficiency for the degradation of 1,4-dioxane by electro-peroxone process. J. Hazard. Mater. 294, 90–98.
Wang, Y.J., Li, X., Zhen, L., Zhang, H., Zhang, Y., Wang, C., 2012. Electro-fenton treatment of concentrates generated in nanofiltration of biologically pretreated landfill leachate. J. Hazard. Mater. 229–230, 115–121.
Weavers, L.K., Ling, F.H., Hoffmann, M.R., 1998. Aromatic compound degradation in water using a combination of sonolysis and ozonolysis. Environ. Sci. Technol. 32 (18), 2727–2733.
Yuan, S., Li, Z.X., Wang, Y.J., 2013. Effective degradation of methylene blue by a novel electrochemically driven process. Electrochem. Commun. 29, 48–51.